Available online at www.sciencedirect.com

ScienceDirect

J. Differential Equations 260 (2016) 4339–4365

Journal of Differential Equations

www.elsevier.com/locate/jde

Nilpotent singularities and dynamics in an SIR type of compartmental model with hospital resources ☆

Chunhua Shan [a], Yingfei Yi [a,c], Huaiping Zhu [b,*]

[a] *Department of Mathematical and Statistical Sciences, University of Alberta, Canada*
[b] *LAMPS and Department of Mathematics and Statistics, York University, Canada*
[c] *School of Mathematics, Jilin University, PR China*

Received 11 March 2015; revised 2 September 2015

Available online 28 November 2015

Abstract

An SIR type of compartmental model with a standard incidence rate and a nonlinear recovery rate was formulated to study the impact of available resources of public health system especially the number of hospital beds. Cusp, focus and elliptic type of nilpotent singularities of codimension 3 are discovered and analyzed in this three dimensional model. Complex dynamics of disease transmission including multi-steady states and multi-periodicity are revealed by bifurcation analysis. Large-amplitude oscillations found in our model provide a more reasonable explanation for disease recurrence. With clinical data, our studies have practical implications for the prevention and control of infectious diseases.

MSC: 34C23; 37G05; 92D30

Keywords: SIR model; Hospital resources; Nonlinear recovery rate; Large-amplitude oscillations; Degenerate Bogdanov–Takens bifurcations; Nilpotent singularities

☆ For this research, Yi is partially supported by NSERC discovery grant 1257749, a faculty development grant from University of Alberta, and a Scholarship from Jilin University. Zhu is partially supported by NSERC and CHIR of Canada and NFSC-11171267, China.
* Corresponding author.
E-mail address: huaiping@mathstat.yorku.ca (H. Zhu).

http://dx.doi.org/10.1016/j.jde.2015.11.009
0022-0396/

1. Introduction

Epidemiological models have been widely used in modeling, control, prevention and prediction of infectious diseases [2,4]. Among numerous epidemiological models, the SIR type of compartmental models and Ross–MacDonald models have been playing a central role in the development of mathematical modeling and analysis of infectious diseases.

The dynamical behaviors of epidemiological models are essentially determined by the demographics of involving populations, the incidence rate and the recovery rate. Let $N(t) = S(t) + I(t) + R(t)$ be the number of the total population, where $S(t)$, $I(t)$ and $R(t)$ are the numbers of susceptible, infectious and recovered individuals at time t, respectively. In classic SIR models, the mass action incidence rate or the standard incidence rate and a linear recovery rate were used. Typically they do not have bistability and periodicity, and the dynamics almost depend on the basic reproduction numbers $\mathbb{R}_0$ [2,4].

However, multiple peaks and recurrence are observed during the transmission of many infectious diseases. Recent studies have shown that the nonlinear incidence rate plays an important role in producing the complex dynamics of epidemic models including oscillations [6,7,12–16, 18] etc.

The per capita recovery rate, μ, is usually considered as a constant in previous modeling. However, in reality it depends on the time of recovering process, which is related to the total infectious individuals seeking treatment as well as available medical resources to the public, denoted by b. Therefore, $\mu = \mu(b, I)$ is a function of both medical resource b and number of infected individuals I. In [17], a simple form of $\mu(b, I)$ was formulated to incorporate the impact of the variation of infectious individuals and available medical resources of health system.

Based on our early work [17], we will further derive and summarize the general properties of the recovery function in section 2, then consider a case where the decreasing function has an inflection point which reflects the critical level of medical resources. Using the new recovery rate μ, we will study the following SIR model with a standard incidence rate

$$\begin{cases} \dfrac{dS}{dt} = A - dS - \dfrac{\beta SI}{S+I+R}, \\ \dfrac{dI}{dt} = -(d+\nu)I - \mu(b,I)I + \dfrac{\beta SI}{S+I+R}, \\ \dfrac{dR}{dt} = \mu(b,I)I - dR, \end{cases} \tag{1.1}$$

where A is the recruitment rate, β is the contact transmission rate, ν is the per capita disease-induced death rate and d is the per capita natural death rate. All the parameters in model (1.1) are positive.

For model (1.1), cusp, focus and elliptic type of nilpotent singularities of codimension 3 shown in Fig. 1 will be discovered and completely analyzed in this paper. Complex dynamics of disease transmission including the disease recurrence are revealed by bifurcation analysis. Concise conditions with geometrical interpretations are derived to classify all the involved bifurcations. Our study shows that the nonlinear recovery rate is an important mechanism in generating complex dynamics. Large-amplitude oscillations found in our model provide a more reasonable explanation for disease recurrence. To the best of our knowledge, this is the first time that focus and elliptic type of Bogdanov–Takens bifurcation of codimension 3 are discovered in epidemic models. This work together with our recent research in [17] could also be the first study

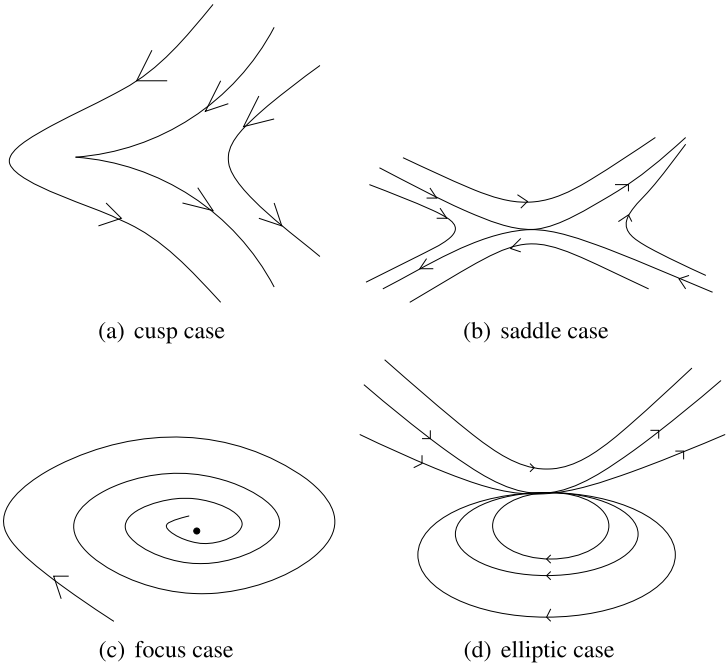

Fig. 1. Different topological types of nilpotent singularities.

of high codimension bifurcations especially the Bogdanov–Takens types of bifurcations in high dimensional biological models.

Nilpotent singularities of high codimension can be the organizing center of complex dynamical systems. There are four types of nilpotent singularities of codimension 3: cusp, nilpotent focus, nilpotent saddle and nilpotent elliptic point as shown in Fig. 1.

The universal unfoldings of these four types of nilpotent singularities of codimension 3 were studied by Dumortier, Roussarie and Sotomayor [8,9]. Some types of the four cases were also studied by Dumortier and Rousseau [10], Xiao [20] and Zoladek [9]. The results on the focus and elliptic cases are still open and a conjecture on the bifurcation diagrams for those cases was proposed in [9]. For the nilpotent saddle and elliptic point, a new normal form was derived by Zhu and Rousseau to treat the cyclicity of nilpotent graphics of saddle or elliptic type [24].

The cusp and saddle types of Bogdanov–Takens bifurcation of codimension 3 were firstly studied in the predator–prey system with a generalized Holling type IV functional response [23] and a generalized Holling type III functional response with prey harvesting [11]. The focus and elliptic types of bifurcations were firstly discovered and studied in a predator–prey system with two Holling types of functional response [22] and a biological model regulated by both disease infection and strong Allee effect [5]. Among the epidemiological models, only the cusp type of Bogdanov–Takens bifurcation of codimension 3 was investigated in an SIRS model with a saturated incidence rate [18] and an SIR model (1.1) with a nonlinear recovery rate [17].

Except the work in [17], high codimension bifurcations, including Bogdanov–Takens bifurcations, were mainly studied in planar systems. In this paper, bifurcation analysis will be carried out in a three dimensional phase space, as system (1.1) cannot be reduced to a planar system by decoupling one variable. We will prove all the involved bifurcations rigorously. The cusp, focus

and elliptic type of Bogdanov–Takens bifurcations of codimension 3 will be identified and studied. During simulations in Fig. 5, we find that existence of nilpotent singularises could be the reason of fast-slow dynamics. To some sense, the results in this paper may be considered as an extension of the work done in [17] in which all the dynamics will be included here.

This paper is organized as follows. In section 2 we formulate the nonlinear recovery rate μ to incorporate the impact of limited medical resources. In section 3 we study the existence and types of the equilibria. In section 4 we study the transcritical bifurcation, saddle-node bifurcation, cusp bifurcation, Hopf bifurcation and Bogdanov–Takens bifurcation of codimension 2, 3 and 4. The codimension 3 bifurcation diagrams near the cusp, nilpotent focus and elliptic point are discussed. Codimension 1 and 2 bifurcation diagrams are presented based on our analytic analysis and simulations. We summarize our results and indicate the epidemiological significance of limited health resources in section 5.

2. SIR model incorporating limited health resources

In classical epidemic models, the per capita recovery rate μ is assumed to be a constant. However, as mentioned above, μ generally depends on the infectious individuals seeking treatment and available medical resources. Therefore, $\mu = \mu(b, I)$ is a function of b and I.

In practice, the hospital bed-population ratio (HBPR), number of available in-patient beds per 10,000 population is used by health planners as an index of estimating resource availability to the public [3,21]. The rationale of using HBPR is explained by WHO Statistical Information System [21] and the data of HBPR in different countries or regions is released annually by WHO in World Health Statistics [21].

In general, for the per capita recovery rate $\mu(b, I)$, we can assume

(A1) $\mu(b, I) > 0$ for $I \geq 0, b > 0$ and $\lim\limits_{I\to 0^+} \mu(b, I) = \mu(b, 0) = \mu_1$, where μ_1 is the maximum per capita recovery rate due to the sufficient medical resources and few infectious individuals.

(A2) $\frac{\partial \mu(b,I)}{\partial I} < 0$, $\lim\limits_{I\to\infty} \mu(b, I) = \mu_0 > 0$. If the number of infectious individuals keeps increasing, the available medical resources cannot meet such large demand for treatment, but a certain number of infectious individuals still can be treated and get recovered, and the minimum recovery rate μ_0 can be obtained.

(A3) $\frac{\partial \mu(b,I)}{\partial b} > 0$, $\lim\limits_{b\to\infty} \mu(b, I) = \mu_1$ and $\lim\limits_{b\to 0^+} \mu(b, I) = \mu_0$. The per capita recovery rate is an increasing function of b.

(A4) $\lim\limits_{I\to 0^+} \dfrac{\partial \mu(b, I)}{\partial I} = 0$ and $\lim\limits_{I\to\infty} \dfrac{\partial \mu(b, I)}{\partial I} = 0$. There will be almost zero rate of the change of μ when the number of infectious is very small or sufficiently large.

(A5) $\frac{\partial^2 \mu(b,I)}{\partial I^2}_{|I=b} = 0$, $\mu(b, I)_{|I=b} = \mu_p \in (\mu_0, \mu_1)$, where $\mu_p = \mu_0 + (\mu_1 - \mu_0)p$ and $p \in (0, 1)$. Comparing the number of infectious and available medical resources, the rate of the change of μ is decreasing when $I < b$ and increasing when $I > b$.

As a preliminary study, a simple form of $\mu(b, I)$ satisfying **(A1)–(A3)** was formulated to incorporate the impact of hospital resources in [17], which is sketched by a blue curve in Fig. 2. However, it is more reasonable to take asymptotic behaviors of $\frac{\partial \mu(b,I)}{\partial I}$ for $I \to 0$ or $I \to \infty$ as well as the relationship between the number of infectious and available hospital resources into consideration as mentioned in **(A4)** and **(A5)**.

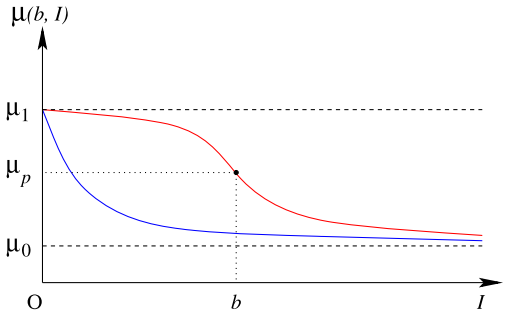

Fig. 2. Curves of per capita recovery rate $\mu(b, I)$ for a given b. (For interpretation of the references to color in this figure, the reader is referred to the web version of this article.)

Generally, according to above assumptions, one can use different functions to formulate the recovery rate, and we study it with a rational function

$$\mu(b, I) = \mu_0 + (\mu_1 - \mu_0)\frac{DI + E}{I^2 + BI + C},$$

where B, C, D and E depending on b and p will be determined under assumptions **(A1)**–**(A5)**.

- By assumptions **(A1)**, $\mu(b, 0) = \mu_1 \Longrightarrow C = E$.
- By assumptions **(A2)** and **(A5)**,

$$0 \le p := \frac{DI + E}{I^2 + BI + C} = \frac{DI + C}{I^2 + BI + C} \le 1, \qquad \forall I \ge 0.$$

  One can argue by contradiction that $B \ge D \ge 0$ and $C > 0$.
- By assumptions **(A4)**, $\lim\limits_{I \to 0^+} \dfrac{\partial \mu(b, I)}{\partial I} = 0 \Longrightarrow B = D$.
- By assumptions **(A5)**, solve B and D in terms of parameters b and p, one can obtain that

$$B = \frac{(1 + \sqrt{1-p})(1 - 2\sqrt{1-p})}{1-p} b \quad \text{and} \quad C = \frac{1 + \sqrt{1-p}}{\sqrt{1-p}} b^2 \text{ where } p \in [\frac{3}{4}, 1).$$

Hence, we determined B, C, D and E, and one can carefully check that all the assumptions are satisfied. Due to the complexity of formulas for B and C, we study a simple form

$$\mu(b, I) = \mu_0 + (\mu_1 - \mu_0)\frac{3b^2}{I^2 + 3b^2}, \tag{2.1}$$

for which $B = D = 0$ and $C = E = 3b^2$ with $p = \frac{3}{4}$.

Therefore we consider system (1.1) with $\mu(b, I)$ defined in (2.1) and initial values

$$S(0) = S_0, I(0) = I_0, R(0) = R_0.$$

Model (1.1) involves seven parameters that all have epidemiological interpretations. By rescaling the state variables and time, we can eliminate some of them. However, we choose not

to because the effect of each of the parameters can be easily seen in our analysis and presentation of results.

A standard argument can be used to show that all solutions initiating in the first octant exist and are eventually bounded by

$$\Sigma = \{(S, I, R) | S \geq 0, I \geq 0, R \geq 0, S + I + R \leq \frac{A}{d}\}.$$

Thus the initial value problem of system (1.1) is epidemiologically reasonable.

3. Existence and types of equilibria

3.1. Existence of equilibria

For system (1.1), one trivial equilibrium is the disease free equilibrium $E_0(\frac{A}{d}, 0, 0)$. Applying the formula in [19], one can calculate the basic reproduction number

$$\mathbb{R}_0 = \frac{\beta}{d + \nu + \mu_1}.$$

For any endemic equilibrium $E(S, I, R)$, its coordinates should satisfy

$$S(I) = \frac{A - [d + \nu + \mu(b, I)]I}{d} > 0, \quad R(I) = \frac{\mu(b, I)I}{d} > 0, \tag{3.1}$$

and I component will be the positive root of the algebraic equation

$$[d + \nu + \mu(b, I)][A + (\beta - \nu)I] - \beta A = 0. \tag{3.2}$$

Lemma 3.1. *If $\beta \leq d + \nu + \mu_0$, there is no endemic equilibria, and E_0 is globally asymptotically stable.*

Proof. For the first part, one can argue it by contradiction. The global stability of E_0 can be proved by constructing Lyapunov function $V = I$ and applying the Lyapunov–Lasalle theorem. □

Now assume $\beta > d + \nu + \mu_0$. Instead of studying Eq. (3.2), we analyze the positive root of an equivalent equation

$$f(I) = \mathscr{A} I^3 + \mathscr{B} I^2 + \mathscr{C} I + \mathscr{D}, \tag{3.3}$$

where

$$\mathscr{A} = (d + \nu + \mu_0)(\beta - \nu), \qquad \mathscr{B} = (d + \nu + \mu_0 - \beta)A,$$
$$\mathscr{C} = 3(d + \nu + \mu_1)(\beta - \nu)b^2, \quad \mathscr{D} = 3(d + \nu + \mu_1)Ab^2(1 - \mathbb{R}_0).$$

Denote Δ_0 the discriminant of $f(I)$ with respect to I, then

$$\Delta_0 = \Delta_0(b) = -3b^2[a_2(\mu_1)b^4 + a_1(\mu_1)b^2 + a_0(\mu_1)],$$

and

$$\begin{aligned}
a_2(\mu_1) &= 36(\beta-\nu)^4\delta_0\delta_1^3,\\
a_1(\mu_1) &= 3A^2(\beta-\nu)^2[(8\delta_0^2+20\delta_0\beta-\beta^2)\delta_1^2 - 18\delta_0\beta(2\delta_0+\beta)\delta_1 + 27\delta_0^2\beta^2],\\
a_0(\mu_1) &= 4A^2(\beta-\delta_0)^3(\beta-\delta_1).
\end{aligned}$$

For the sake of simplicity, the notations $\delta_i = d+\nu+\mu_i$ for $i=1,2$ are introduced.

Define an auxiliary function

$$g(b) = a_2(\mu_1)b^4 + a_1(\mu_1)b^2 + a_0(\mu_1).$$

In order to study the roots of Eq. (3.3), it is necessary to study the roots of function $g(b)$.

Let $\Delta_1(\mu_1)$ be the discriminant of $g(b)$ with respect b^2, and a straightforward calculation leads that

$$\Delta_1(\mu_1) = 9A^4\beta(\beta-\nu)^4(\delta_1-\delta_0)(\delta_1\beta+8\delta_0\delta_1-9\delta_0\beta)^3.$$

Let

$$\delta_1^* = \frac{9\delta_0\beta}{8\delta_0+\beta} \quad \text{and} \quad \mu_1^* = \frac{9\delta_0\beta}{8\delta_0+\beta} - d - \nu,$$

then

$$\Delta_1(\mu_1) = 0 \Longleftrightarrow \delta_1 = \delta_1^* \Longleftrightarrow \mu_1 = \mu_1^*.$$

Two potential positive roots of $\Delta_0(b) = 0$ are

$$b = b^-(\mu_1) = \sqrt{\frac{-a_1(\mu_1) - \sqrt{\Delta_1(\mu_1)}}{2a_2(\mu_1)}},\ b = b^+(\mu_1) = \sqrt{\frac{-a_1(\mu_1) + \sqrt{\Delta_1(\mu_1)}}{2a_2(\mu_1)}}.$$

Lemma 3.2. *$a_1(\mu_1) < 0$ for $\forall \mu_1 \in [\,\mu_1^*, \beta-d-\nu]$.*

Proof. Since $\delta_0 < \beta$, we have $\mu_1^* < \beta - d - \nu$.

Let $\tilde{g}(\delta_1) = \dfrac{a_1(\mu_1)}{3A^2(\beta-\nu)^2}$, a quadratic function of δ_1. One can check that

$$\begin{aligned}
&\tilde{g}(\delta_0) = 8\delta_0^2(\beta-\delta_0)^2 > 0, \quad \tilde{g}(\delta_1^*) = -\frac{216\beta^2\delta_0^2(\beta-\delta_0)^2}{(\beta+8\delta_0)^2} < 0,\\
&\tilde{g}(\beta) = -\beta^2(\beta-\delta_0)^2 < 0, \quad g(+\infty) = +\infty.
\end{aligned}$$

By continuity, $\tilde{g}(\delta_1) < 0$ for $\forall \delta_1 \in [\delta_1^*, \beta]$, i.e., $a_1(\mu_1) < 0$ for $\forall \mu_1 \in [\,\mu_1^*, \beta-d-\nu]$. □

For $b = b^{\pm}(\mu_1)$, we have the following two lemmas.

Lemma 3.3. *$b = b^-(\mu_1)$ is defined for $\mu_1 \in [\ \mu_1^*,\ \beta - d - \nu]$, and $b = b^+(\mu_1)$ is defined for $\mu_1 \in [\ \mu_1^*,\ +\infty)$. Furthermore, $b^-(\mu_1) \le b^+(\mu_1)$ whenever they are defined, and $b^-(\mu_1) = b^+(\mu_1)$ iff $\mu_1 = \mu_1^*$.*

Proof. By definitions of $b^\pm(\mu_1)$, we require $\Delta_1(\mu_1) \ge 0$. In fact, one can find that

$$\Delta_1(\mu_1) \ge 0 \Longleftrightarrow \mu_1 \ge \mu_1^*.$$

We distinguish the following two cases and analyze functions $b = b^\pm(\mu_1)$.

(1) $\mu_1 > \beta - d - \nu$.

We have $a_0(\mu_1) < 0$. Note that $a_2(\mu_1) > 0$ is always true. Therefore,

$$\Delta_1(\mu_1) = a_1^2(\mu_1) - 4a_2(\mu_1)a_0(\mu_1) > a_1^2(\mu_1).$$

Hence, for $\mu_1 \in (\beta - d - \nu, +\infty)$, $b = b^+(\mu_1)$ is well defined while $b = b^-(\mu_1)$ is not defined.

(2) $\mu_1^* \le \mu_1 \le \beta - d - \nu$.

By Lemma 3.2, we have $a_1(\mu_1) < 0$. Note that $a_2(\mu_1) > 0$ and $a_0(\mu_1) \ge 0$.

Again, by definitions of $b = b^\pm(\mu_1)$, we have that $b = b^\pm(\mu_1)$ are well defined for $\mu_1 \in [\mu_1^*,\ \beta - d - \nu]$. Furthermore, $b^+(\mu_1) \ge b^-(\mu_1) \ge 0$ and $b^-(\mu_1) = b^+(\mu_1)$ iff $\mu_1 = \mu_1^*$, $b^-(\mu_1) = 0$ iff $\mu_1 = \beta - d - \nu$. □

Lemma 3.4. *For the functions $b = b^\pm(\mu_1)$,*

(1). $\dfrac{\partial b^\pm(\mu_1)}{\partial \mu_1} < 0, \quad \dfrac{\partial b^-(\mu_1^*)}{\partial \mu_1} = \dfrac{\partial b^+(\mu_1^*)}{\partial \mu_1}.$

(2). $\lim\limits_{\mu_1 \to \beta - d - \nu} \dfrac{\partial b^-(\mu_1)}{\partial \mu_1} = -\infty, \quad \lim\limits_{\mu_1 \to \infty} \dfrac{\partial b^+(\mu_1)}{\partial \mu_1} = 0.$

Proof. By straightforward calculations. □

Denote

$$b^* = b^\pm(\mu_1^*) = \frac{1}{9}\frac{(\beta - \delta_0)A}{(\beta - \nu)\delta_0}\sqrt{\frac{\beta + 8\delta_0}{\beta}} \quad \text{and} \quad b_K = \frac{\sqrt{3}}{6}\frac{(\beta - \delta_0)A}{(\beta - \nu)\delta_0}\sqrt{\frac{\delta_0}{\beta}}.$$

For the existence of endemic equilibria, we are ready to present the following theorem.

Theorem 3.5. *Suppose $\beta > d + \nu + \mu_0$. Three curves*

$$\begin{aligned} &C_0 : \mu_1 = \beta - d - \nu, && b > 0, \\ &C_\Delta^- : b = b^-(\mu_1), && \mu_1 \in [\mu_1^*, \beta - d - \nu], \\ &C_\Delta^+ : b = b^+(\mu_1), && \mu_1 \in [\mu_1^*, \infty), \end{aligned}$$

divide the region $\mu_1 > \mu_0$, $b > 0$ into 4 subregions V_0, V_1, V_2 and V_3 (see Fig. 3):

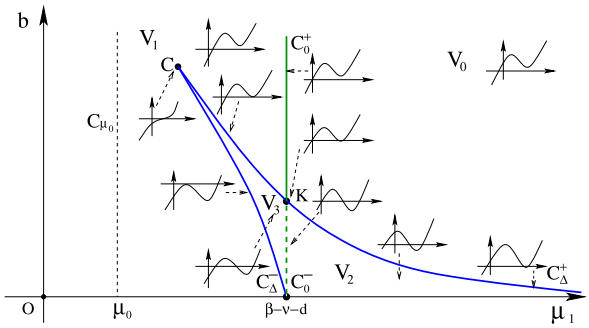

Fig. 3. Bifurcation curves in (μ_1, b) plane when $\beta > d + \nu + \mu_0$. There will be 0, 1, 2 and 3 simple endemic equilibria in regions V_0, V_1, V_2 and V_3, respectively. A saddle-node bifurcation occurs across $C_\Delta^\pm$, and a transcritical bifurcation occurs across $C_0^- \cup K \cup C_0^+$.

$$
\begin{aligned}
V_0 &= \{(\mu_1, b) | \mu_1 > \beta - d - \nu, \quad b > b^+(\mu_1)\},\\
V_1 &= \{(\mu_1, b) | \mu_0 < \mu_1 < \beta - d - \nu, \quad b > 0\} \setminus cl V_3,\\
V_2 &= \{(\mu_1, b) | \mu_1 > \beta - d - \nu, \quad 0 < b < b^+(\mu_1)\},\\
V_3 &= \{(\mu_1, b) | \mu^* < \mu_1 < \beta - d - \nu, \quad b^-(\mu_1) < b < b^+(\mu_1)\}.
\end{aligned}
$$

In regions V_0, V_1, V_2 and V_3, system has 0, 1, 2 and 3 simple endemic equilibria, respectively.

1. *Along $C_0 = C_0^- \cup K \cup C_0^+$, where $K = (\beta - d - \nu, b_K)$*
   - *if $b > b_K$: no endemic equilibria;*
   - *if $b = b_K$: an endemic equilibrium of multiplicity 2;*
   - *if $b < b_K$: two simple equilibria.*
2. *Along C_Δ^-: a simple endemic equilibrium and an endemic equilibrium of multiplicity 2.*
3. *Along C_Δ^+,*
   - *if $\mu_1^* < \mu_1 < \beta - d - \nu$: a simple endemic equilibrium and an endemic equilibrium of multiplicity 2;*
   - *if $\mu_1 \geq \beta - d - \nu$: an endemic equilibrium of multiplicity 2.*
4. *At the point $C(\mu_1^*, b^*)$: an endemic equilibrium of multiplicity 3.*

Remark 3.6. $\mathbb{R}_0 = 1$ defines the straight line C_0 in (μ_1, b) plane.

From now on we denote any endemic equilibrium as $E(\bar{S}, \bar{I}, \bar{R})$. Let E_1, E_2 and E_3 be the three simple endemic equilibria whenever they exist, whose corresponding I components satisfy $I_1 < I_2 < I_3$. For example, E_1 is the unique endemic equilibrium in V_1, and E_2 and E_3 are the two equilibria in V_2.

3.2. Types of equilibria

Theorem 3.7. *For system (1.1), the disease free equilibrium $E_0(\frac{A}{d}, 0, 0)$ is*

- $\mathbb{R}_0 < 1$*: an attracting node;*
- $\mathbb{R}_0 > 1$*: a hyperbolic saddle;*
- $\mathbb{R}_0 = 1$*: a saddle-node of codimension 1.*

Proof. For system (1.1), $-d$, $-d$ and $(d+\nu+\mu_1)(\mathbb{R}_0-1)$ are three eigenvalues of Jacobian at E_0. If $\mathbb{R}_0<1$, E_0 is an attracting node. If $\mathbb{R}_0>1$, E_0 is a hyperbolic saddle.

If $\mathbb{R}_0=1$, the third eigenvalue is zero. To determine the type of E_0, we linearize system (1.1) at E_0, diagonalize the linear part and on the center manifold we have

$$\dot{X}=-\frac{(\beta-\nu)\beta d}{Ab^2}X^2+\mathcal{O}(X^3). \tag{3.4}$$

Hence, E_0 is a saddle-node of codimension 1. □

Theorem 3.8. *For system (1.1), suppose that $E(\bar{S},\bar{I},\bar{R})$ is a simple endemic equilibrium, i.e. $f(\bar{I})=0$ and $f'(\bar{I})\neq 0$, then E is a hyperbolic saddle if $f'(\bar{I})<0$ and an anti-saddle if $f'(\bar{I})>0$.*

Proof. The Jacobian at any endemic equilibrium E is given by

$$J(E)=\begin{pmatrix} -d-\dfrac{\beta\bar{I}(\bar{I}+\bar{R})}{(\bar{S}+\bar{I}+\bar{R})^2} & -\dfrac{\beta\bar{S}(\bar{S}+\bar{R})}{(\bar{S}+\bar{I}+\bar{R})^2} & \dfrac{\beta\bar{S}\bar{I}}{(\bar{S}+\bar{I}+\bar{R})^2} \\ \dfrac{\beta\bar{I}(\bar{I}+\bar{R})}{(\bar{S}+\bar{I}+\bar{R})^2} & -\mu'(b,\bar{I})\bar{I}-\dfrac{\beta\bar{S}\bar{I}}{(\bar{S}+\bar{I}+\bar{R})^2} & -\dfrac{\beta\bar{S}\bar{I}}{(\bar{S}+\bar{I}+\bar{R})^2} \\ 0 & \mu'(b,\bar{I})\bar{I}+\mu(b,\bar{I}) & -d \end{pmatrix}.$$

For simplicity, sometimes we write $\mu(b,I)$ as μ or $\mu(I)$ and $\frac{\partial\mu(b,I)}{\partial I}$ as μ' or $\mu'(b,I)$. One can verify $\lambda=-d$ is always an eigenvalue, and the other two eigenvalues of $J(E)$ are the roots of

$$\lambda^2-\mathcal{T}(\bar{I})\lambda+\mathcal{D}(\bar{I})=0, \tag{3.5}$$

where

$$\mathcal{T}(\bar{I})=\frac{6(\mu_1-\mu_0)b^2\bar{I}^2}{(\bar{I}^2+3b^2)^2}-\frac{d[A+(\beta-\nu)\bar{I}]}{A-\nu\bar{I}} \quad\text{and}\quad \mathcal{D}(\bar{I})=\frac{d\,\bar{I}f'(\bar{I})}{(A-\nu\bar{I})(\bar{I}^2+3b^2)}.$$

Hence, E is a hyperbolic saddle if $f'(\bar{I})<0$ and E is an anti-saddle if $f'(\bar{I})>0$. Here $\lambda=-d$ is not taken into account. □

4. Bifurcations

4.1. Bifurcation of singularities

Theorem 4.1. *Consider $\mathbb{R}_0$ as the bifurcation parameter. When $\mathbb{R}_0=1$, system (1.1) undergoes a forward bifurcation. The backward bifurcation will never occur. However, the disease could persist even if $\mathbb{R}_0<1$.*

Proof. $\mathbb{R}_0$ depends on parameters β, d, ν and μ_1. Without loss of generality, we choose μ_1 as the bifurcation parameter.

Let $\mu_1 = \beta - d - \nu + \varepsilon$ and substitute μ_1 into the system (1.1). One can linearize the system (1.1) at E_0 and diagonalize the linear part, then apply the center manifold theorem with the parameter ε, and obtain the following reduced system on the center manifold

$$\dot{X} = -\left(\varepsilon + O(\varepsilon^2)\right) X - \left(\frac{(\beta-\nu)\beta d}{Ab^2} + O(\varepsilon)\right) X^2 + O(X^3). \tag{4.1}$$

Denote the right side of system (4.1) as $F(X, \varepsilon)$. Since

$$F(0,0) = F_X(0,0) = F_\varepsilon(0,0) = 0, \quad F_{X\varepsilon}(0,0) = -1, \quad F_{XX}(0,0) = -\frac{(\beta-\nu)\beta d}{Ab^2} \neq 0,$$

system (4.1) undergoes a transcritical bifurcation.

Since $\frac{\partial \mathbb{R}_0}{\partial \varepsilon}|_{\varepsilon=0} = -\frac{1}{\beta} < 0$, system (1.1) undergoes a forward bifurcation when $\mathbb{R}_0 = 1$ from the epidemiological point of view. Even though the backward bifurcation will never occur, the disease could persist for $\mathbb{R}_0 < 1$ by Theorem 3.5 and Fig. 3. □

Theorem 4.2. *Assume $\mathcal{T}(\bar{I}) \neq 0$.*

- *When $f(\bar{I}) = f'(\bar{I}) = 0$ and $f''(\bar{I}) \neq 0$, the endemic equilibrium of multiplicity 2 is a saddle-node of codimension 1. When $b = b^{\pm}(\mu_1)$, system (1.1) undergoes a saddle-node bifurcation.*
- *When $f(\bar{I}) = f'(\bar{I}) = f''(\bar{I}) = 0$, the endemic equilibrium of multiplicity 3 is a semi-hyperbolic point of codimension 2. When $(\mu_1, b) = (\mu_1^*, b^*)$, system (1.1) undergoes a cusp bifurcation.*

The unfolding of the semi-hyperbolic point of codimension 2 *is given in the bifurcation diagram of Fig. 3 in terms of parameters μ_1 and b.*

Proof. Firstly we prove the second part of this theorem.

If $f(\bar{I}) = f'(\bar{I}) = f''(\bar{I}) = 0$, three equilibria E_1, E_2 and E_3 coalesce at one point E. One can find that 0, $\mathcal{T}(\bar{I})$ and $-d$ are three eigenvalues of $J(E)$ with associated eigenvectors $\overline{V}_1|_{I=\bar{I}}$, $\overline{V}_2|_{I=\bar{I}}$ and $\overline{V}_3|_{I=\bar{I}}$, where

$$\overline{V}_1 = \begin{pmatrix} -(\mu' I + d + \nu + \mu) \\ d \\ \mu' I + \mu \end{pmatrix}, \overline{V}_2 = \begin{pmatrix} \beta - d - \frac{\beta(\mu+2d)I}{A-\nu I} \\ \mu' I + \frac{d\beta I}{A-\nu I} \\ -(\mu' I + \mu) \end{pmatrix}, \overline{V}_3 = \begin{pmatrix} \frac{A-(d+\nu+\mu)}{(d+\mu)I} \\ 0 \\ 1 \end{pmatrix}.$$

We derive the normal form on the one dimensional center manifold as follows.

The translation $x = S - \bar{S}$, $y = I - \bar{I}$ and $z = R - \bar{R}$ brings E to the origin. Let

$$\begin{pmatrix} x \\ y \\ z \end{pmatrix} = T \begin{pmatrix} X \\ Y \\ Z \end{pmatrix}, \qquad T = (\overline{V}_1, \overline{V}_2, \overline{V}_3)\Big|_{I=\bar{I}}.$$

Under the transformation T which diagonalizes the Jacobian $J(E)$, system (1.1) becomes

$$\begin{cases} \dot{X} = \sum\limits_{i,j,k\in\mathbb{N}}^{i+j+k=2,3} l_{ijk} X^i Y^j Z^k + \mathcal{O}(|X,Y,Z|^4), \\ \dot{Y} = \mathcal{T}(\bar{I})Y + \sum\limits_{i,j,k\in\mathbb{N}}^{i+j+k=2} m_{ijk} X^i Y^j Z^k + \mathcal{O}(|X,Y,Z|^3), \\ \dot{Z} = -dZ + \sum\limits_{i,j,k\in\mathbb{N}}^{i+j+k=2} n_{ijk} X^i Y^j Z^k + \mathcal{O}(|X,Y,Z|^3). \end{cases} \tag{4.2}$$

We choose not to present l_{ijk}, m_{ijk} and n_{ijk} here. By algebraic simplification, we have

$$l_{200} = *f''(\bar{I}) = 0,$$

where $*$ denotes a function of parameters. Therefore, we need to compute the center manifold.

For $X \sim 0$, there exists a center manifold

$$Y = -\frac{m_{200}}{\mathcal{T}(\bar{I})}X^2 + O(X^3), \qquad Z = \frac{n_{200}}{d}X^2 + O(X^3). \tag{4.3}$$

System (4.2) reduced on the one dimensional center manifold (4.3) is given by

$$\begin{aligned} \dot{X} &= \left(l_{300} - \frac{l_{110}m_{200}}{\mathcal{T}(\bar{I})} + \frac{l_{101}n_{200}}{d}\right)X^3 + O(X^4) \\ &= \frac{1}{4}\frac{27(\beta-\nu)^3 d^3 \delta_0^3}{(\beta-\delta_0)(2\delta_0+\beta)A^2[(\delta_0-\nu)\beta + 2(\beta-\nu)\delta_0]\mathcal{T}(\bar{I})}X^3 + O(X^4). \end{aligned}$$

The coefficient of X^3 is defined and does not vanish. Hence E is a semi-hyperbolic point of codimension 2.

As a direct consequence of cusp bifurcation, if $f(\bar{I}) = f'(\bar{I}) = 0$, $f''(\bar{I}) \neq 0$, immediately we know that the system on the center manifold is topologically equivalent to

$$\dot{X} = \pm X^2 + O(X^3).$$

Therefore, it is a saddle-node of codimension 1. □

4.2. Hopf bifurcation

We introduce the following lemma which is useful when presenting bifurcation diagrams in $(\mathbb{R}_0, I)$ plane and proving the transversality condition of Hopf bifurcations.

Lemma 4.3. *(1). If* $\mathbb{R}_0 > 1$, $\inf\limits_{b>0} I(b) = \dfrac{(\beta-\delta_1)A}{(\beta-\nu)\delta_1}$ *and* $\sup\limits_{b>0} I(b) = \dfrac{(\beta-\delta_0)A}{(\beta-\nu)\delta_0}$.

(2). For $i = 1, 2, 3$, *we have*

$$(-1)^{i+1}\frac{\partial I_i}{\partial \mu_1} < 0, \ \forall \mu_1 > 0 \quad \text{and} \quad (-1)^{i+1}\frac{\partial I_i}{\partial b} < 0, \ \forall b > 0. \tag{4.4}$$

(3). $\mathcal{T}(I) = 0$ *has at most two positive roots.*

Proof. (1) Any positive root of $f(I) = 0$ is the I-component of the intersection of two curves

$$y = f_1(I) = (\beta - \nu)\delta_0 I^3 + (\delta_0 - \beta)AI^2,$$
$$y = f_2(I) = -3b^2[(\beta - \nu)\delta_1 I + (\delta_1 - \beta)A].$$

We can argue it by the geometric characteristic of these two curves.

(2) Obviously we have $(-1)^{i+1}\frac{\partial f}{\partial I_i} > 0$. Applying the implicit function theorem to Eq. (3.3), one can obtain that

$$\frac{\partial I_i}{\partial \mu_1} = -\frac{\partial f}{\partial \mu_1}/\frac{\partial f}{\partial I_i}, \qquad \frac{\partial I_i}{\partial b} = -\frac{\partial f}{\partial b}/\frac{\partial f}{\partial I_i}.$$

Note that $\frac{\partial f}{\partial \mu_1} = 3b^2[(\beta - \nu)I_i + A] > 0$, so $(-1)^{i+1}\frac{\partial I_i}{\partial \mu_1} < 0$.

We claim that $\frac{\partial f}{\partial b} = 6b[(\beta - \nu)\delta_1 I_i + (\delta_1 - \beta)A] > 0$, so $(-1)^{i+1}\frac{\partial I_i}{\partial b} < 0$.

In fact, if $\mathbb{R}_0 \le 1$, then $\delta_1 \ge \beta$, obviously $\frac{\partial f}{\partial b} > 0$; If $\mathbb{R}_0 > 1$, by part (1) of this lemma, $I_i \ge \inf_{b>0} I(b)$. Therefore, we have $\frac{\partial f}{\partial b} > 0$.

(3) Let $\mathcal{T}(I) = t_1(I) - t_2(I)$, where

$$y = t_1(I) = \frac{6(\mu_1 - \mu_0)b^2 I^2}{(I^2 + 3b^2)^2}, \quad y = t_2(I) = \frac{d[A + (\beta - \nu)I]}{A - \nu I}.$$

Again, we can argue it by the geometric characteristic of these two curves. See Fig. 4 (a). □

Denote two potential positive roots of $\mathcal{T}(I) = 0$ as H_m and H_M, where $H_m \le H_M$.

Theorem 4.4. *A generic Hopf bifurcation could occur if $I_i = H_m$, $I_i = H_M$ or $I_i = H_m = H_M$ for $i = 1, 3$.*

Proof. We only have to verify the transversality condition. Let $\gamma = \frac{\mathcal{T}(I_i)}{2}$ be the real part of the pair of the complex eigenvalues of the characteristic equation (3.5).

If $I_i = H_M$ or $I_i = H_m = H_M$, we consider μ_1 as the bifurcation parameter and fix all the other parameters. Suppose there exists a $\hat{\mu}_1$ such that $\mathcal{T}(I_i(\hat{\mu}_1), \hat{\mu}_1) = 0$, then

$$\frac{d\gamma}{d\mu_1}\Big|_{\mu_1=\hat{\mu}_1} = \frac{1}{2}\left(\frac{\partial \mathcal{T}(I_i(\mu_1), \mu_1)}{\partial I_i}\frac{\partial I_i(\mu_1)}{\partial \mu_1} + \frac{\partial \mathcal{T}(I_i(\mu_1), \mu_1)}{\partial \mu_1}\right)\Big|_{\mu_1=\hat{\mu}_1}.$$

Furthermore,

$$\frac{\partial \mathcal{T}(I_i(\mu_1), \mu_1)}{\partial I_i}\Big|_{\mu_1=\hat{\mu}_1} \le 0, \qquad \frac{\partial \mathcal{T}(I_i(\mu_1), \mu_1)}{\partial \mu_1}\Big|_{\mu_1=\hat{\mu}_1} = \frac{6b^2 H_M}{(H_M^2 + 3b^2)^2} > 0.$$

By part (2) of Lemma 4.3, we have $\frac{d\gamma}{d\mu_1}\Big|_{\mu_1=\hat{\mu}_1} > 0$.

If $I_i = H_m$, we consider b as the bifurcation parameter and fix all the other parameters. Suppose there exists a $\hat{b}$ such that $\mathcal{T}(I_i(\hat{b}), \hat{b}) = 0$, then

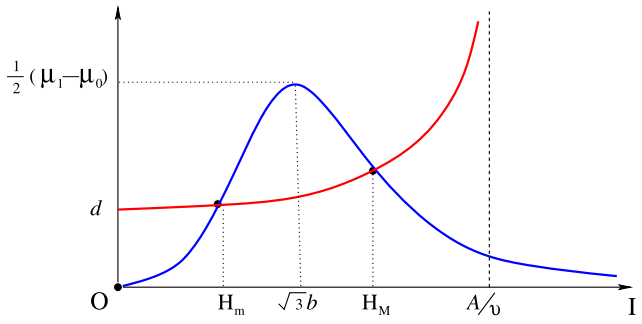

(a) Intersections of $y = t_i(I)$

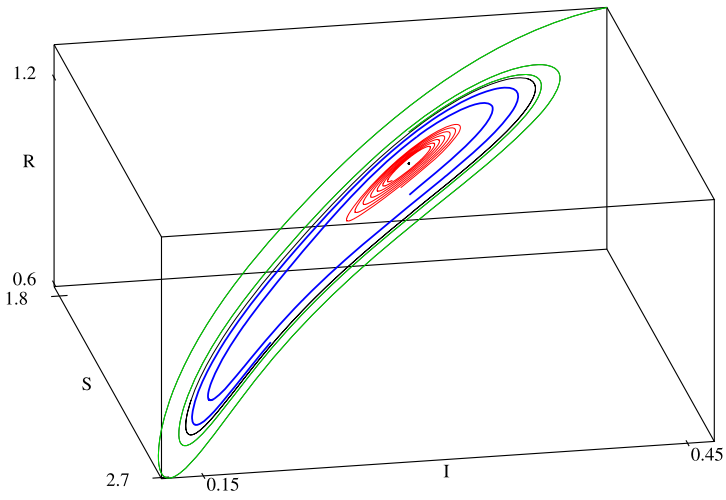

(b) Two limit cycles

Fig. 4. (a) Intersections of $y = t_1(I)$ and $y = t_2(I)$; (b) Two limit cycles bifurcate from a focus. The outer one with black color is stable and the inner one lying between the blue and red curves on the center manifold is unstable. $A = 20$, $\mu_0 = 10$, $d = 5.8$, $\nu = 1$, $\beta = 42.6471$, $\mu_1 = 29.8$ and $b = 0.165$. (For interpretation of the references to color in this figure legend, the reader is referred to the web version of this article.)

$$\frac{d\gamma}{db}\Big|_{b=\hat{b}} = \frac{1}{2}\left(\frac{\partial \mathcal{T}(I_i(b),b)}{\partial I_i}\frac{\partial I_i(b)}{\partial b} + \frac{\partial \mathcal{T}(I_i(b),b)}{\partial b}\right)\Big|_{b=\hat{b}}.$$

Furthermore,

$$\frac{\partial \mathcal{T}(I_i(b),b)}{\partial I_i}\Big|_{b=\hat{b}} > 0, \qquad \frac{\partial \mathcal{T}(I_i(b),b)}{\partial b}\Big|_{b=\hat{b}} = \frac{12(\mu_1-\mu_0)\hat{b}^2H_m^2(H_m^2-3\hat{b}^2)}{(H_m^2+3\hat{b}^2)^3} < 0.$$

By part (2) of Lemma 4.3, we have $\dfrac{d\gamma}{db}\Big|_{b=\hat{b}} < 0$. □

Let l_n be the nth Lyapunov coefficient of the focus E_1 or E_3. In order to prove the existence of a generic Hopf bifurcation, in addition to the transversality condition, one also needs to verify that the first Lyapunov coefficient $l_1 \neq 0$.

As will be shown in section 4.3, the Bogdanov–Takens (BT) bifurcation of codimension 3 occurs. It has been proven in [8,9] that the cusp, focus and elliptic types of BT bifurcations of codimension 3 will guarantee the existence of a Hopf bifurcation of codimension 2 ($l_1 = 0$, $l_2 \neq 0$) in a small neighborhood of BT singularities of codimension 3 in the parameter space. An example showing that two limit cycles bifurcated from the degenerate Hopf bifurcation is given in Fig. 4 (b).

Without calculation of l_1, immediately one can have the following three cases for system (1.1):

(1) $l_1 < 0$: supercritical Hopf bifurcation;
(2) $l_1 > 0$: subcritical Hopf bifurcation;
(3) $l_1 = 0$: degenerate Hopf bifurcation. Moreover, Hopf bifurcation is of codimension 2 in a small neighborhood of BT singularities of codimension 3 in the parameter space [8,9].

Therefore, in Theorem 4.4, we only need to check the transversality condition, because there will exist some region in the parameter space in which the condition $l_1 \neq 0$ can be obtained. Also we choose not to present l_1 here due to its complexity.

The codimension of a degenerate Hopf bifurcation is an interesting topic if it occurs far from the BT singularities in the parameter space. In order to give a complete analysis of Hopf bifurcation, one at least has to compute the second Lyapunov coefficient for this system which is rather complicated. We leave it for future work.

4.3. Bogdanov–Takens bifurcations

We will study Bogdanov–Takens bifurcations of codimension 2, 3 and 4 in this section.

Theorem 4.5. *Suppose*

$$f(\bar{I}) = f'(\bar{I}) = \mathcal{T}(\bar{I}) = 0, \quad f''(\bar{I}) \neq 0 \quad \text{and} \quad \mathcal{T}'(\bar{I}) \neq 0,$$

system (1.1) localized at E is topologically equivalent to

$$\begin{cases} \dot{X} = Y, \\ \dot{Y} = sgn(f''(\bar{I}))X^2 - sgn(\mathcal{T}'(\bar{I}))XY + \mathcal{O}(|X, Y|^3), \end{cases} \tag{4.5}$$

so E is a Bogdanov–Takens point of codimension 2.

Proof. Firstly bring E to the origin by the translation $x = S - \bar{S}$, $y = I - \bar{I}$, $z = R - \bar{R}$. Let

$$\begin{pmatrix} x \\ y \\ z \end{pmatrix} = T \begin{pmatrix} X \\ Y \\ Z \end{pmatrix}, \qquad T = (\overline{V}_1, \widetilde{V}_2, \overline{V}_3)\Big|_{I=\bar{I}},$$

where $\widetilde{V}_2 = (-1, 1, 0)'$ and $|T| = -\frac{d(A-\nu\bar{I})^2}{\beta(d+\mu)\bar{I}^2} < 0$. Hence, system (1.1) becomes

$$\begin{cases} \dot{X} = Y + \sum\limits_{i,j,k\in\mathbb{N}}^{i+j+k=2} l_{ijk} X^i Y^j Z^k + \mathcal{O}(|X,Y,Z|^3), \\ \dot{Y} = \sum\limits_{i,j,k\in\mathbb{N}}^{i+j+k=2} m_{ijk} X^i Y^j Z^k + \mathcal{O}(|X,Y,Z|^3), \\ \dot{Z} = -dZ + \sum\limits_{i,j,k\in\mathbb{N}}^{i+j+k=2} n_{ijk} X^i Y^j Z^k + \mathcal{O}(|X,Y,Z|^3), \end{cases} \tag{4.6}$$

where l_{200}, m_{200} and m_{110} have the same form as those in [17] if we do not distinguish $\mu(b, I)$, $\mu'(b, I)$ and $|T|$ in each case.

For $X, Y \sim 0$, there exists a center manifold $Z = \mathcal{O}(|X, Y|^2)$ on which we have

$$\begin{cases} \dot{X} = Y + L_{20}X^2 + L_{11}XY + L_{02}Y^2 + \mathcal{O}(|X,Y|^3), \\ \dot{Y} = M_{20}X^2 + M_{11}XY + M_{02}Y^2 + \mathcal{O}(|X,Y|^3), \end{cases} \tag{4.7}$$

where $L_{ij} = l_{ij0}$ and $M_{ij} = m_{ij0}$ for $0 \le i + j \le 2$. Using the near-identity transformation

$$\begin{aligned} X &= u + \frac{1}{2}(L_{11} + M_{02})u^2 + L_{02}uv + \mathcal{O}(|u,v|^3), \\ Y &= v - L_{20}u^2 + M_{02}uv + \mathcal{O}(|u,v|^3), \end{aligned}$$

and rewriting u, v into X, Y, we obtain

$$\begin{cases} \dot{X} = Y, \\ \dot{Y} = \overline{M}_{20}X^2 + \overline{M}_{11}XY + \mathcal{O}(|X,Y|^3), \end{cases} \tag{4.8}$$

where $\overline{M}_{20} = m_{200}$ and $\overline{M}_{110} = 2l_{200} + m_{110}$.

Now determine signs of $\overline{M}_{20}$ and $\overline{M}_{11}$. By algebraic simplification, we can find that

$$\begin{aligned} \operatorname{sgn}\left(\overline{M}_{20}\right) &= -\operatorname{sgn}\Big([d + \nu + \mu(b,I)][A + (\beta - \nu)I]\Big)''_{|I=\bar{I}} = -\operatorname{sgn}\Big(f''(\bar{I})\Big), \\ \operatorname{sgn}\left(\overline{M}_{11}\right) &= -\operatorname{sgn}\Big((\mu' I) + \Big[\frac{d(A + (\beta - \nu)I)}{(A - \nu I)^2}\Big]\Big)'_{|I=\bar{I}} = \operatorname{sgn}\Big(\mathcal{T}'(\bar{I})\Big). \end{aligned}$$

By assumptions $f''(\bar{I}) \neq 0$ and $\mathcal{T}'(\bar{I}) \neq 0$, making a change of coordinates and time to preserve the orientation by time

$$X \to -\Big|\frac{\overline{M}_{20}}{\overline{M}_{11}^2}\Big|X, \quad Y \to -\Big|\frac{\overline{M}_{20}^2}{\overline{M}_{11}^3}\Big|Y, \quad t \to \Big|\frac{\overline{M}_{11}}{\overline{M}_{20}}\Big|t,$$

then system (4.8) is topologically equivalent to system (4.5). □

Theorem 4.6. *Suppose that*

$$f(\bar{I}) = f'(\bar{I}) = \mathcal{T}(\bar{I}) = 0,$$

(1). If $f''(\bar{I}) = 0$ *and* $\mathcal{T}'(\bar{I}) \neq 0$, *E is a nilpotent focus/elliptic point;*
(2). If $f''(\bar{I}) = 0$ *and* $\mathcal{T}'(\bar{I}) = 0$, *E is a nilpotent focus;*
(3). If $f''(\bar{I}) \neq 0$ *and* $\mathcal{T}'(\bar{I}) = 0$, *E is a cusp point.*
The codimension of all the nilpotent singularities are greater than or equal to 3.

Proof. From Theorem 4.5, if $f''(\bar{I})\mathcal{T}'(\bar{I}) \neq 0$ fails, the Bogdanov–Takens bifurcation will be degenerate. To identify its type, we need to study system (4.8) up to $\mathcal{O}(|X, Y|^4)$, and this procedure can be accomplished as follows.
Step 1. Expand system (4.6) up to $\mathcal{O}(|X, Y, Z|^4)$.
Step 2. Calculate the center manifold

$$Z = h(X, Y) = \sum_{i,j\in\mathbb{N}}^{i+j=2,3} h_{ij} X^i Y^j + \mathcal{O}(|X, Y|^4)$$

and reduce system (4.6) on the center manifold, then we obtain

$$\begin{cases} \dot{X} = Y + \sum\limits_{2\leq i+j\leq 4} L_{ij} X^i Y^j + \mathcal{O}(|X, Y|^5), \\ \dot{Y} = \sum\limits_{2\leq i+j\leq 4} M_{ij} X^i Y^j + \mathcal{O}(|X, Y|^5). \end{cases} \tag{4.9}$$

Step 3. Make a near-identity transformation to eliminate non-resonant terms in (4.9), then

$$\begin{cases} \dot{X} = Y, \\ \dot{Y} = \sum\limits_{i=2,3,4} \left(\overline{M}_{i0} X^i + \overline{M}_{i-1,1} X^{i-1} Y \right) + \mathcal{O}(X^5) + \mathcal{O}(|X, Y|^4) Y. \end{cases} \tag{4.10}$$

Due to the complexity, we choose not to present the center manifold and the near-identity transformation here.

To simplify the analysis and presentation, we change the parameters

$$\overline{F} : (\mu_1, \mu_0, b, d, \nu, \beta, A) \longrightarrow (\delta_1, \delta_0, b, d, \nu, \beta, A)$$

for $\delta_i = \mu_i + d + \nu$. One can check that $\overline{F}$ is bijective.

Now we consider $(\delta_1, \delta_0, b, d, \nu, \beta, A)$ instead of $(\mu_1, \mu_0, b, d, \nu, \beta, A)$ as independent parameters, and recall that $\min\{\delta_1, \beta\} > \delta_0 > d + \nu$.

We break down our analysis in three cases.
(1). $f''(\bar{I}) = 0, \mathcal{T}'(\bar{I}) \neq 0$.

From $f''(\bar{I}) = 0$, we have $\bar{I} = \frac{A(\beta-\delta_0)}{3\delta_0(\beta-\nu)}$. By assumptions $f(\bar{I}) = f'(\bar{I}) = \mathcal{T}(\bar{I}) = 0$, solving for parameters δ_1, b and d, one can obtain

$$\delta_1 = \delta_1^*, b = b^*, d = d^* = \frac{3\delta_0\beta(\beta-\delta_0)[(\delta_0-\nu)\beta+2(\beta-\nu)\delta_0]}{(\beta-\nu)(\beta+2\delta_0)^3}.$$

Consequently, we present $\overline{M}_{i0}$ and $\overline{M}_{i-1,1}$ by the other four parameters β, ν, δ_0 and A. Hence,

$$\begin{aligned}
&\overline{M}_{20} = 0,\\
&\overline{M}_{11} = \frac{27\beta^2\delta_0^3(\beta-\delta_0)(\beta+2\delta_0)}{A(\beta+2\delta_0)^6}\left[(\beta-4\delta_0)\nu - \frac{3\beta\delta_0(2\beta-5\delta_0)}{(\beta+2\delta_0)}\right],\\
&\overline{M}_{30} = -\frac{729}{4}\frac{(\beta-\delta_0)^2\beta^4\delta_0^6[(\delta_0-\nu)\beta+2(\beta-\nu)\delta_0]^2}{A^2(\beta+2\delta_0)^{10}} < 0.
\end{aligned}$$

Denote $\nu_* = \frac{3\beta\delta_0(2\beta-5\delta_0)}{(\beta+2\delta_0)(\beta-4\delta_0)}$, then $\mathcal{T}'(\bar{I}) \neq 0$ if and only if $\nu \neq \nu_*$.

$\overline{M}_{21}$, $\overline{M}_{40}$ and $\overline{M}_{31}$ are complex and not presented here. Let

$$\nu_\pm = \frac{\beta^3+2\beta^2\delta_0+11\delta_0^2\beta+4\delta_0^3 \pm \sqrt{\Delta_3}}{2(\beta+2\delta_0)^2},$$

where $\Delta_3 = (\beta-\delta_0)^2(\beta^4+2\delta_0\beta^3+33\delta_0^2\beta^2+56\delta_0^3\beta+16\delta_0^4)$. One can check that $0 < \nu_- < \nu_+$. Since $\delta_0 > d+\nu$, we need to have $\nu \in (\nu_-, \nu_+)$.

Step 4. Eliminating the term $\mathcal{O}(X^4)$ in system (4.10).

Let $\phi(x) = \overline{M}_{30}x^3 + \overline{M}_{40}x^4 + \mathcal{O}(x^5)$. By a change of coordinates and time

$$X \to \left(-4\int_0^X \phi(x)dx\right)^{\frac{1}{4}}, Y \to -Y, \quad t \to \left(-4\int_0^X \phi(x)dx\right)^{-\frac{3}{4}} \phi(X)t,$$

we obtain

$$\begin{cases} \dot{X} = Y,\\ \dot{Y} = -X^3 + Y\left[\dfrac{-\overline{M}_{11}}{\sqrt{-\overline{M}_{30}}}X + \dfrac{(-\overline{M}_{30})^{-\frac{7}{4}}Q}{5}X^2 + \mathcal{O}(X^3)\right], \end{cases}$$

where

$$Q = 5\overline{M}_{30}\overline{M}_{21} - 3\overline{M}_{40}\overline{M}_{11} = -\frac{177\,147}{16}\frac{\delta_0^{11}\beta^7(\beta-\delta_0)^3[(\delta_0-\nu)\beta+2(\beta-\nu)\delta_0]}{(\beta+2\delta_0)^{20}A^4}\psi(\nu),$$

and

$$\begin{aligned}
\psi(\nu) = {}& (\beta+2\delta_0)^3(13\beta^2+124\delta_0\beta+16\delta_0^2)\nu^3\\
&+\beta(\beta+2\delta_0)^2(4\beta^3-111\delta_0\beta^2-1194\delta_0^2\beta-76\delta_0^3)\nu^2\\
&-3\beta^2\delta_0(\beta+2\delta_0)(8\beta^3-129\delta_0\beta^2-1224\delta_0^2\beta-32\delta_0^3)\nu-81\beta^4\delta_0^3(46\delta_0+5\beta).
\end{aligned}$$

Step 5. Determine $Sign(\overline{M}_{11}^2 + 8\overline{M}_{30})$.

The sign of $\overline{M}_{11}^2 + 8\overline{M}_{30}$ distinguishes elliptic and focus types of singularities, which has the following expression

$$\overline{M}_{11}^2 + 8\overline{M}_{30} = -\frac{729\beta^4\delta_0^6(\beta-\delta_0)^2(\beta^2+16\delta_0\beta-8\delta_0^2)\,[(\nu-\nu_1)(\nu-\nu_2)]}{A^2(\beta+2\delta_0)^{10}},$$

where $\nu_1 < \nu_2$ with $\nu_1 = \frac{3\sqrt{2}}{2}\frac{[(9\sqrt{2}+14)\delta_0-2\beta]\beta\delta_0}{[(8+6\sqrt{2})\delta_0+\beta](\beta+2\delta_0)}$ and $\nu_2 = \frac{3\sqrt{2}}{2}\frac{[(9\sqrt{2}-14)\delta_0+2\beta]\beta\delta_0}{[(8-6\sqrt{2})\delta_0+\beta](\beta+2\delta_0)} > 0$.

Now define $J = (\nu_-, \nu_+) \setminus \{\nu_*\}$. We classify the types of singularities in terms of parameter $\nu \in J$. Define

$$\begin{aligned}
J_1 &= \{\nu \in J \setminus J_4 | \nu \in ((0, \max(0, \nu_1)) \cup (\nu_2, +\infty))\},\\
J_2 &= \{\nu \in J \setminus J_4 | \nu \in (\max(0, \nu_1), \nu_2)\},\\
J_3 &= \{\nu \in J | \nu = \nu_i, i = 1, 2\},\\
J_4 &= \{\nu \in J | \psi(\nu) = 0\}.
\end{aligned}$$

Therefore, according to [1,9,24] we have

- $\nu \in J_1$, E is a nilpotent focus of codimension 3. See Fig. 5 (a).
- $\nu \in J_2$, E is a nilpotent elliptic point of codimension 3. See Fig. 5 (b).
- $\nu \in J_3$, E is a nilpotent elliptic point of codimension at least 4, type 1.
- $\nu \in J_4$, E is a nilpotent focus/elliptic point of codimension at least 4, type 2.

(2). $f''(\bar{I}) = \mathcal{T}'(\bar{I}) = 0$.

By assumptions $f(\bar{I}) = f'(\bar{I}) = \mathcal{T}(\bar{I}) = 0$, solve for parameters δ_1, b, d and ν, then

$$\delta_1 = \frac{9\beta\delta_0}{\beta+8\delta_0}, b = \frac{(\beta+2\delta_0)(\beta-4\delta_0)A\sqrt{\beta(8\delta_0+\beta)}}{9\delta_0(\beta-7\delta_0)\beta^2}, d = \frac{9\delta_0^2\beta(\beta-\delta_0)}{(7\delta_0-\beta)(\beta+2\delta_0)^2}, \nu = \frac{3\beta\delta_0(2\beta-5\delta_0)}{(\beta+2\delta_0)(\beta-4\delta_0)}.$$

We present $\overline{M}_{30}$ and $\overline{M}_{21}$ by the other three parameters β, δ_0 and A.

$$\begin{aligned}
&\overline{M}_{20} = 0, \quad \overline{M}_{11} = 0,\\
&\overline{M}_{30} = -\frac{6561}{4}\frac{(\beta-\delta_0)^4\beta^6\delta_0^8}{A^2(\beta+2\delta_0)^{10}(\beta-4\delta_0)^2} < 0,\\
&\overline{M}_{21} = -\frac{2187}{4}\frac{(\beta-\delta_0)^3\beta^5\delta_0^7(7\beta^2-8\delta_0\beta+64\delta_0^2)}{A^2(\beta+2\delta_0)^{10}(\beta-4\delta_0)^2} < 0.
\end{aligned}$$

Therefore, it is a more degenerate nilpotent focus [1]. See Fig. 5 (d). The codimension of this singularity is at least 4, and the unfolding and bifurcation studies of this nilpotent focus are still open.

(3). $f''(I) \neq 0, \mathcal{T}'(\bar{I}) = 0$.

In this case, E is a cusp point at least codimension 3 [8]. See Fig. 5 (c). In order to determine its codimension, we need to determine $Sign(\overline{M}_{31}\overline{M}_{20} - \overline{M}_{30}\overline{M}_{21})$ as we did in [17], where the exact codimension of cusp point was studied, and it was of codimension 3. The computation of $\overline{M}_{31}\overline{M}_{20} - \overline{M}_{30}\overline{M}_{21}$ is much more complex than the first two cases because we cannot derive explicit expression of three parameters in terms of the other four. The dynamics near the codimension 3 cusp point will be similar to those presented in [17]. The study of exact codimension of this cusp is beyond our scope. □

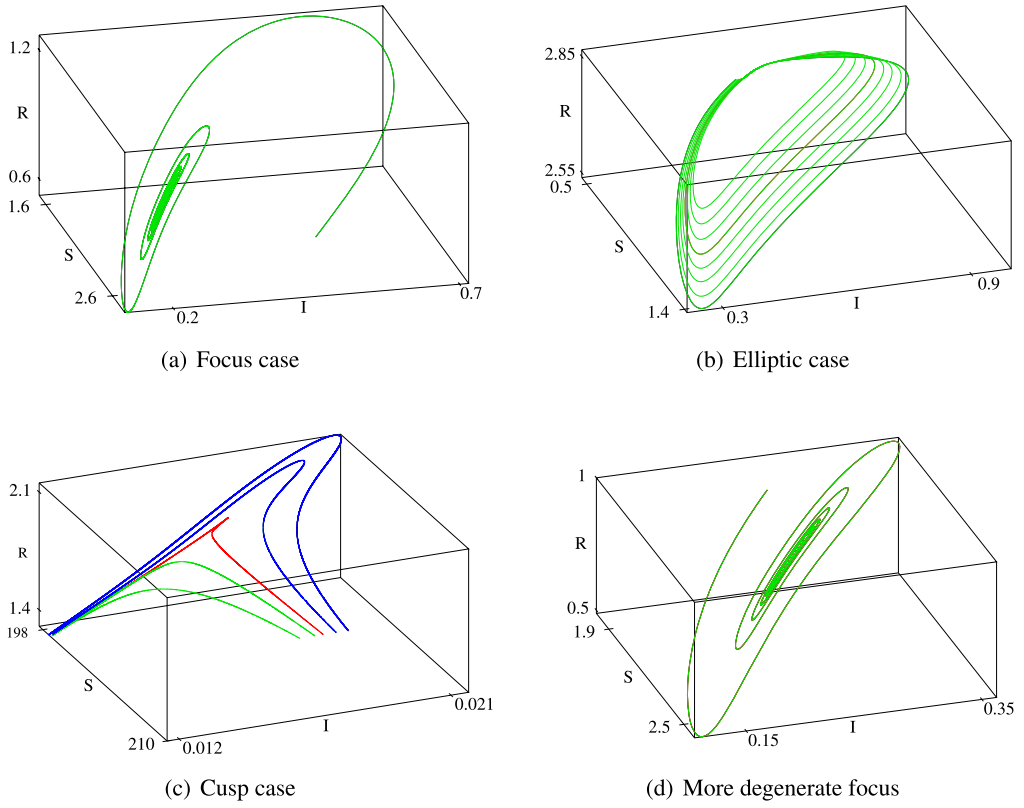

(a) Focus case (b) Elliptic case

(c) Cusp case (d) More degenerate focus

Fig. 5. Types of degenerate Bogdanov–Takens points.

Remark 4.7. J_i $(i = 1, 2, 3, 4)$ are nonempty sets, and all the types of nilpotent singularities mentioned in Theorem 4.6 exist. See some numerical examples in Fig. 5. Values of parameters are given to 5 decimal places for cases (a)–(d) in Fig. 5.

(a) $A = 20$, $\nu = 1$, $\mu_0 = 10$, $d = 5.8$, $\beta = 39.73177$, $\mu_1 = 27.69941$, $b = 0.16395$;
(b) $A = 20$, $\nu = 1$, $\mu_0 = 6.32569$, $d = 4.674308$, $\beta = 168$, $\mu_1 = 63.05296$, $b = 0.21685$;
(c) $A = 20$, $\nu = 1$, $\mu_0 = 10$, $d = 0.1$, $\beta = 11.30342$, $\mu_1 = 10.20200$, $b = 0.01025$;
(d) $A = 20$, $\nu = 1$, $\mu_0 = 10$, $d = 6.24291$, $\beta = 42.64708$, $\mu_1 = 29.40488$, $b = 0.16177$.

We summary Theorems 3.8, 4.2, 4.4, 4.5 and 4.6 in the following tables.

Theorem 4.8.

Conditions	*Types of bifurcations*	*Codimension*
$f(\bar{I}) = 0, f'(\bar{I}) \neq 0, \mathcal{T}(\bar{I}) \neq 0$	*Hyperbolic*	0
$f(\bar{I}) = f'(\bar{I}) = 0, f''(\bar{I}) \neq 0, \mathcal{T}(\bar{I}) \neq 0$	*Saddle-node*	1
$f(\bar{I}) = f'(\bar{I}) = f''(\bar{I}) = 0, \mathcal{T}(\bar{I}) \neq 0$	*Cusp*	2
$f(\bar{I}) = 0, f'(\bar{I}) > 0, \mathcal{T}(\bar{I}) = 0$	*Hopf*	≥ 2

Suppose that $f(\bar{I}) = f'(\bar{I}) = \mathcal{T}(\bar{I}) = 0$, *then*

Conditions		*Types of BT bifurcations*	*Codimension*
$f''(\bar{I})\mathcal{T}'(\bar{I}) < 0$		*Subcritical cusp*	2
$f''(\bar{I})\mathcal{T}'(\bar{I}) > 0$		*Supercritical cusp*	2
$f''(\bar{I}) \neq 0, \mathcal{T}'(\bar{I}) = 0$		*Cusp type*	≥ 3
$f''(\bar{I}) = 0, \mathcal{T}'(\bar{I}) \neq 0$	$\nu \in J_1$	*Focus*	3
	$\nu \in J_2$	*Elliptic*	3
	$\nu \in J_3$	*Elliptic, type 1*	≥ 4
	$\nu \in J_4$	*Focus/elliptic, type 2*	≥ 4
$f''(\bar{I}) = \mathcal{T}'(\bar{I}) = 0$		*Focus*	≥ 4

4.4. Unfoldings and bifurcation diagrams

We focus on the bifurcations with codimension less than or equal to 3.

We wish to study system (1.1) for parameters (δ_1, b, d) in a neighborhood of (δ_1^*, b^*, d^*) and $\nu \in J_1$ (or $\nu \in J_2$). Thus let

$$\delta_1 = \delta_1^* + \varepsilon_1, \quad b = b^* + \varepsilon_2, \quad d = d^* + \varepsilon_3$$

in model (1.1), and we obtain a perturbed system

$$\begin{cases} \dot{S} = A - (d^* + \varepsilon_3)S - \dfrac{\beta SI}{S + I + R}, \\ \dot{I} = -[\delta_0 + \dfrac{3(\delta_1^* + \varepsilon_1 - \delta_0)(b^* + \varepsilon_2)^2}{I^2 + 3(b^* + \varepsilon_2)^2}]I + \dfrac{\beta SI}{S + I + R}, \\ \dot{R} = [\delta_0 - d^* - \varepsilon_3 - \nu + \dfrac{3(\delta_1^* + \varepsilon_1 - \delta_0)(b^* + \varepsilon_2)^2}{I^2 + 3(b^* + \varepsilon_2)^2}]I - (d^* + \varepsilon_3)R, \end{cases} \tag{4.11}$$

for sufficiently small parameters $(\varepsilon_1, \varepsilon_2, \varepsilon_3)$.

Theorem 4.9. *For parameters* $\varepsilon = (\varepsilon_1, \varepsilon_2, \varepsilon_3)$ *sufficiently small and* $\nu \in J_1$ *(*$\nu \in J_2$*), system (4.11) is a generic unfolding of focus (elliptic) singularity of codimension 3.*

Proof. This proof is extremely long but standard and we only give the main idea here. One has to show that system (4.11) can be brought to the following normal form (4.12) up to C^∞ equivalence.

$$\begin{cases} \dot{x} = y, \\ \dot{y} = \xi_1 + \xi_2 x - x^3 + y(\xi_3 + \bar{b}(\xi)x + x^2) + y^2 W(x, y, \xi), \end{cases} \tag{4.12}$$

where $\bar{b}$ is C^∞ in ξ and W is C^∞ in (x, y, ξ).

One may refer to [9] for the general procedure. Firstly we apply step 1 in Theorem 4.6 to system (4.11). Compute the center manifold depending on parameters

$$Z = h(X, Y) = \sum_{i,j\in\mathbb{N}}^{0\le i+j\le 3} h_{ij}(\varepsilon) X^i Y^j + \mathcal{O}(|X, Y|^4),$$

and reduce the system to a planar system. Similar to steps 2, 3 and 4 introduced in Theorem 4.6, by a sequence of coordinate changes depending on the parameter $(\varepsilon_1, \varepsilon_2, \varepsilon_3)$, we obtain the normal form (4.12) where (ξ_1, ξ_2, ξ_3) is a function of $(\varepsilon_1, \varepsilon_2, \varepsilon_3)$.

For each step, one should keep in mind that the computations should agree with those in each step of Theorem 4.6 when $\varepsilon = 0$.

Finally we check the following non-degeneracy property,

$$\frac{\partial(\xi_1, \xi_2, \xi_3)}{\partial(\varepsilon_1, \varepsilon_2, \varepsilon_3)}_{|(0,0,0)} = \frac{(\beta + 8\delta_0)A^2(\beta - \nu)^2(\beta + 2\delta_0)^6\sqrt{\beta(\beta + 8\delta_0)}}{843\,750 \cdot \beta^2\delta_0^4[(\delta_0 - \nu)\beta + 2(\beta - \nu)\delta_0]^4} \frac{Q^6}{(-\overline{M}_{30})^{\frac{21}{2}}} \neq 0.$$

Hence we finish the proof. □

The bifurcation diagrams for the cusp, focus and elliptic point of codimension 3 were studied and given by Dumortier, Roussarie and Sotomayor [8,9]. By Theorem 4.9, system (4.11) has the same bifurcation set with respect to $(\varepsilon_1, \varepsilon_2, \varepsilon_3)$ as system (4.12) has with respect to (ξ_1, ξ_2, ξ_3), up to a homeomorphism in the parameter space. Since $\frac{\partial \overline{F}(\mu_1,\mu_0,b,d,\nu,\beta,A)}{\partial(\mu_1,\mu_0,b,d,\nu,\beta,A)} = 1$, system (1.1) has the same bifurcation set with respect to (μ_1, b, d) in a small neighborhood of $(\delta_1^* - d^* - \nu, b^*, d^*)$ as system (4.12) has with respect to (ξ_1, ξ_2, ξ_3) up to a homeomorphism.

Remark 4.10. One may plot the bifurcation diagram on (μ_1, b) plane near the singularity of codimension 3. This can be achieved by taking slice with each fixed d near $(\delta_1^* - d^* - \nu, b^*, d^*)$. A numerical example is given in Fig. 6 which is one slice near the nilpotent focus of codimension 3. Note that this is an incomplete bifurcation diagram because three branches of homoclinic curves are hard to trace due to the numerical difficulties.

Remark 4.11. By the bifurcation analysis of high codimension nilpotent singularities, the mechanism of the occurrence of limit cycles may fall into the following categories.

(a). Limit cycles may appear and disappear from Hopf bifurcation.

(b). Limit cycles may appear from Hopf bifurcation and disappear from Homoclinic bifurcation (vice verse).

(c). Limit cycles may appear from Hopf bifurcation and disappear from saddle-node bifurcation of limit cycles (vice verse).

(d). Limit cycles may appear from Homoclinic bifurcation and disappear from saddle-node bifurcation of limit cycles (vice verse).

(e) Limit cycles may appear and disappear from saddle-node bifurcation of limit cycles.

In epidemiology, much more attention has been paid to the relationship between $\mathbb{R}_0$ and the number of the infectious, so it is preferable to plot the bifurcation diagram on $(\mathbb{R}_0, I)$ plane.

Let $\mathbb{R}_{0i} = \mathbb{R}_{0|b=b_i(\mu_1), b\neq b_i(\mu_1^*)}$, $i = 1, 2$. By Theorems 3.5, 4.2 and part (2) of Lemma 4.3 we obtain the bifurcation diagram in Fig. 7. Note that the equilibria E_1 and E_3 in Fig. 7 may lose stability due to Hopf bifurcation and limit cycles will be present. Refer to Fig. 8 for some numerical examples where limit cycles are involved in the $(\mathbb{R}_0, I)$ bifurcation diagram.

In this section, we fix $A = 20, \mu_0 = 10, d = 5.8, \nu = 1, \beta = 42.6471$ in all simulations.

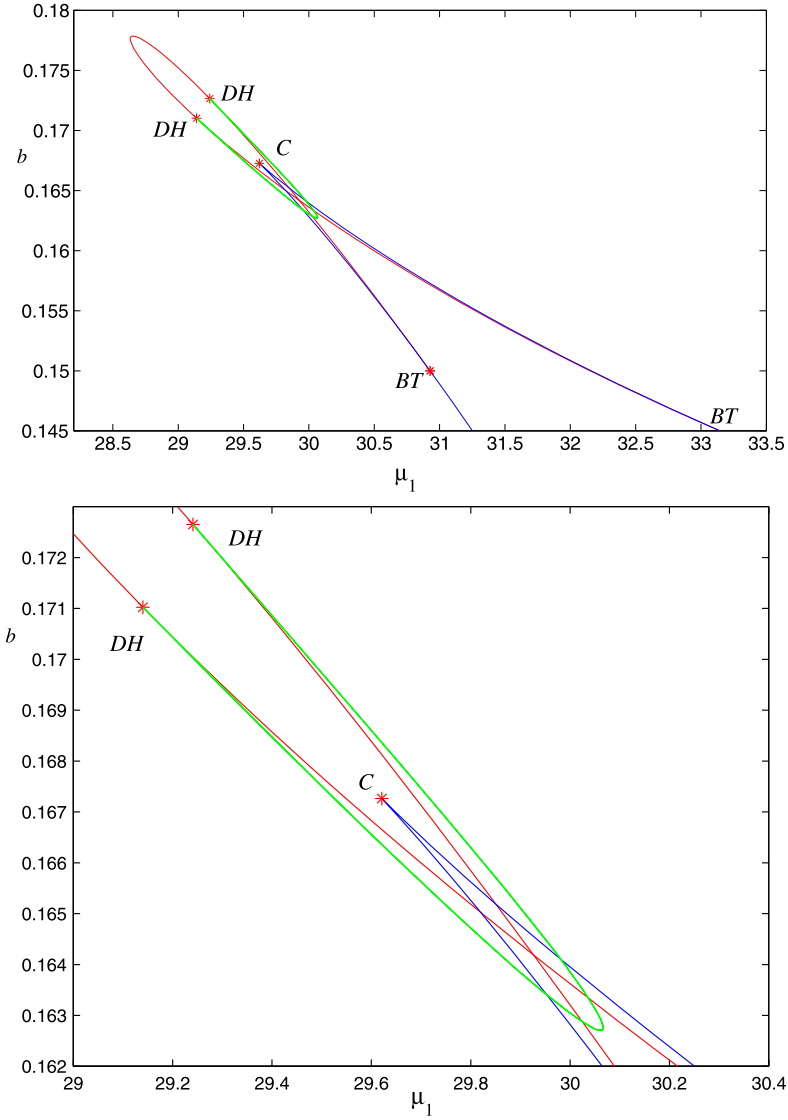

Fig. 6. A slice of codimension 3 bifurcation diagram near a nilpotent focus. C, BT and DH denote cusp bifurcation point, Bogdanov–Takens bifurcation point and degenerate Hopf bifurcation point, respectively. Blue, red and green lines are saddle-node bifurcation, Hopf bifurcation and saddle-node bifurcation of limit cycles curves. We magnify the small neighborhood of C in the right figure. (For interpretation of the references to color in this figure legend, the reader is referred to the web version of this article.)

Remark 4.12. The periodic solution generated from Hopf bifurcation has a small amplitude near the equilibrium which is common in epidemic models. However, limit cycles with a large amplitude make more sense but are rarely seen. The large limit cycle enclosing three equilibria, guaranteed by the focus type of Bogdanov–Takens bifurcation, implies the disease recurrence of large-amplitude. See Fig. 8 (c) and (d). In particular, there are two large limit cycles for $\mathbb{R}_0 \sim 1.1581$ or $\mathbb{R}_0 \sim 1.1605$ in Fig. 8 (d).

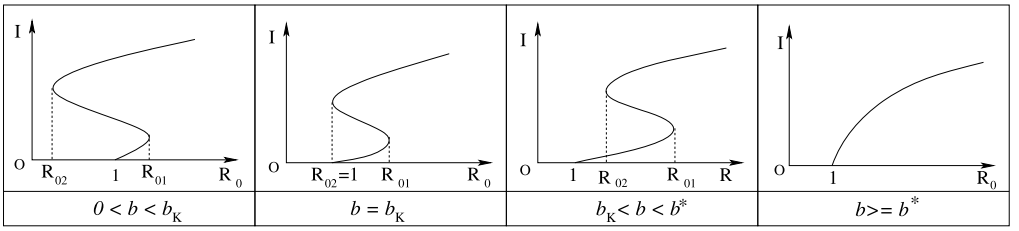

Fig. 7. Bifurcation of equilibria with the parameter $\mathbb{R}_0$. A transcritical bifurcation occurs when $\mathbb{R}_0 = 1$ and a saddle-node bifurcation occurs when $\mathbb{R}_0 = \mathbb{R}_{0i}$. Equilibria E_1, E_2 and E_3 are represented by the lower, middle and upper branch of the curves. There will be no hysteresis behavior when $b \geq b^*$.

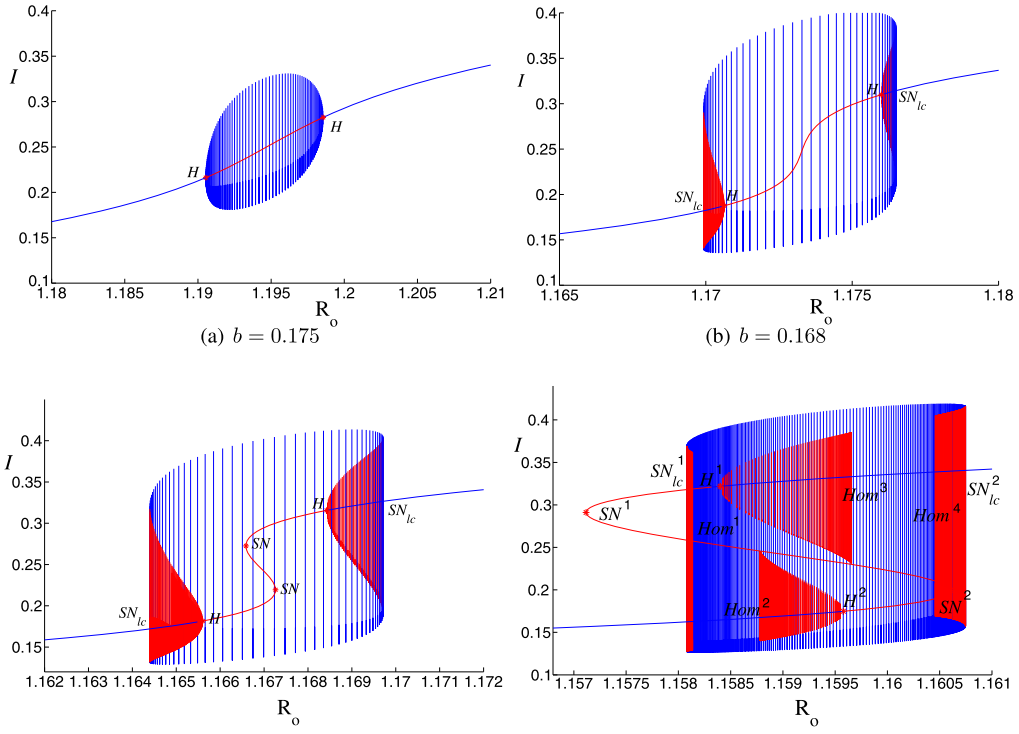

Fig. 8. Bifurcation diagram on $(\mathbb{R}_0, I)$ plane with different b. Blue (red) curves represent the stable (unstable) singularities or limit cycles. H, Hom, SN and SN_{lc} denote Hopf bifurcation, homoclinic bifurcation, saddle-node bifurcation and saddle-node bifurcation of limit cycles. (For interpretation of the references to color in this figure legend, the reader is referred to the web version of this article.)

As shown in Fig. 8 (d), dynamics of system (1.1) are still extremely complicated, even if we only change one parameter and fix all the other parameters. In Fig. 9, we plot 18 types of phase portraits in the two dimensional center manifold appearing in Fig. 8 (d) for $\mathbb{R}_0$ varying from 1 to $\beta/(d + \nu + \mu_0)$. For notations in Fig. 9, for instance, $[H^2, Hom^3)$, it means $\mathbb{R}_{0|H^2} \leq \mathbb{R}_0 < \mathbb{R}_{0|Hom^3}$. We use blue (red, purple) curves to represent stable (unstable, semi-stable) limit cycles

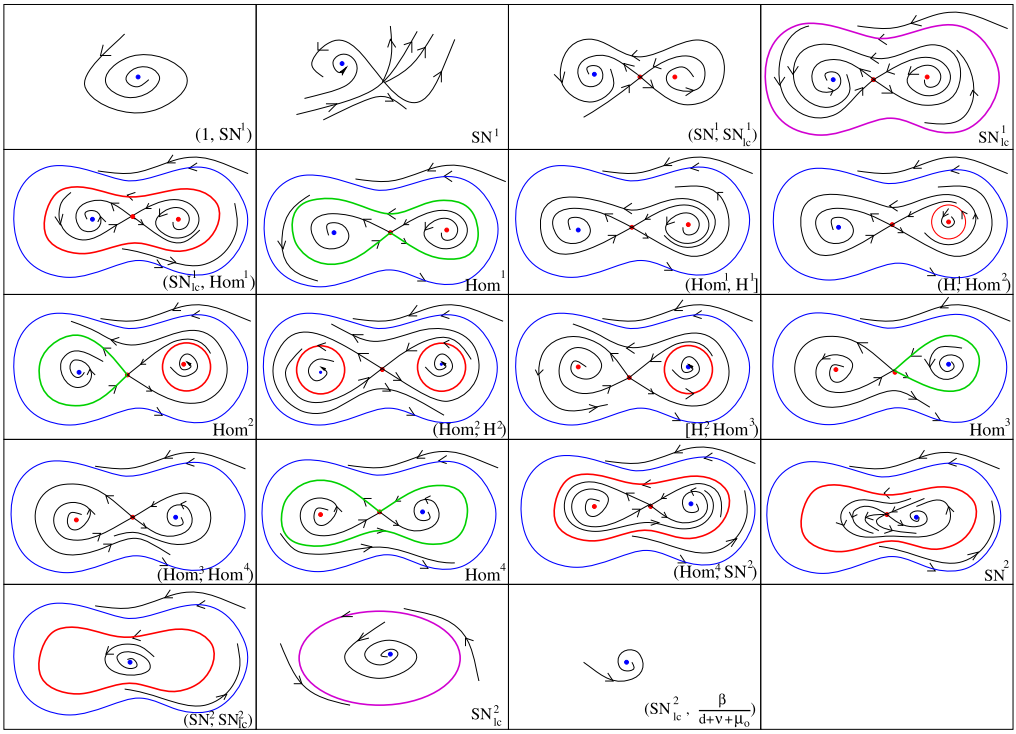

Fig. 9. Phase Portraits of Fig. 8 (d) in 2d center manifold as $\mathbb{R}_0$ varies. (For interpretation of the references to color in this figure, the reader is referred to the web version of this article.)

in Fig. 9. The saddle loops are represented by green curves. One can easily observe the evolution of topological structure of system (1.1) as $\mathbb{R}_0$ varies.

5. Discussions and applications

In [17] three factors, demographics of populations, standard incidence rate and nonlinear impact of limit health resources, determine the complex dynamics of system (1.1). Different from the study in [17], the nonlinear recovery rate considered here has two independent ingredients, characterized by an inflection point, which affects dynamics of (1.1) dramatically and generates even higher codimension singularities.

The corresponding SIR model with a constant per capita recovery rate was studied by Mena-Lorca and Hethcote [15]. They showed that dynamics of the model completely depend on $\mathbb{R}_0$. In contrast to their work and classic epidemic models, this paper together with our previous study in [17] reveal that $\mathbb{R}_0$ is not enough to determine the dynamical behaviors, and the nonlinear recovery rate can play an important role in generating complex dynamics.

The impact of limited health resources on disease transmission is studied in Lemma 4.3, Theorems 3.5, 4.2, 4.4 and 4.6 and illustrated in Figs. 3, 6, 7 and 8. As we see, limited health resources impact the dynamics of the system significantly. We summary it as follows.

• It is the one of the parameters unfolding the high codimension bifurcations. Therefore, a small variation of b will result in the change of the topological structure of the system.

• The periodic solution with a small amplitude cannot be present if b is sufficiently large. This is because $\mathcal{T}(\bar{I}) < 0$ for a large b which yields that the Hopf bifurcation cannot occur.

• Recall Lemma 4.3 that

$$(-1)^{i+1}\frac{\partial I_i}{\partial b} < 0 \text{ for } i = 1, 3 \text{ and } \inf_{b>0} I(b) = \frac{(\beta - \delta_1)A}{(\beta - \nu)\delta_1} > 0 \text{ if } \mathbb{R}_0 > 1.$$

Hence, increasing the amount of health resources can only reduce limited number of the infectious, but cannot eliminate the disease when $\mathbb{R}_0 > 1$.

• If $\mathbb{R}_0 < 1$, from Theorem 4.1, we can eliminate the disease when

$$b > b^+(\mu_1) = \sqrt{\frac{-a_1(\mu_1) + \sqrt{\Delta_1(\mu_1)}}{2a_2(\mu_1)}}. \tag{5.1}$$

The mathematical results in this paper are applicable to the control, prevention and prediction of disease transmission. Large-amplitude oscillations found in our model provide a more reasonable explanation for disease recurrence. Our results can help the public health agencies arrange the appropriate amount of health resources to prevent disease outbreak. For a specific disease, our study suggests that maintaining a certain amount of health resources, which can be estimated by clinical or historical data, is crucial for the prevention and control of infectious diseases.

Acknowledgments

The authors thank the referee for careful reading and comments which help to improve our paper.

References

[1] A. Andronov, E. Leontovich, I. Gordon, A. Maier, Theory of Bifurcations of Dynamical Systems on a Plane, Israel Program for Scientific Translations, Jerusalem, 1971.
[2] R.M. Anderson, R.M. May, Infectious Diseases of Humans: Dynamics and Control, Oxford University Press, Oxford, New York, 1991.
[3] R. Boaden, N. Proudlove, M. Wilson, An exploratory study of bed management, J. Manag. Med. 13 (1999) 234–250.
[4] F. Brauer, C. Castillo-Chávez, Mathematical Models in Population Biology and Epidemiology, Springer-Verlag, New York, 2001.
[5] L. Cai, G. Chen, D. Xiao, Multiparametric bifurcations of an epidemiological model with strong Allee effect, J. Math. Biol. 67 (2013) 185–215.
[6] V. Capasso, G. Serio, A generalization of the Kermack–Mckendrick deterministic epidemic model, Math. Biosci. 42 (1978) 43–61.
[7] W.R. Derrick, P. van den Driessche, A disease transmission model in a nonconstant population, J. Math. Biol. 31 (1993) 495–512.
[8] F. Dumortier, R. Roussarie, J. Sotomayor, Generic 3-parameter families of vector fields on the plane, unfolding a singularity with nilpotent linear part: the cusp case of codimension 3, Ergodic Theory Dynam. Systems 7 (1987) 375–413.
[9] F. Dumortier, R. Roussarie, J. Sotomayor, H. Zoladek, Bifurcations of Planar Vector Fields, Nilpotent Singularities and Abelian Integrals, Lecture Notes in Mathematics, vol. 1480, Springer-Verlag, Berlin, 1991.
[10] F. Dumortier, C. Rousseau, Cubic Liénard equations with linear damping, Nonlinearity 3 (1990) 1015–1039.
[11] R. Etoua, C. Rousseau, Bifurcation analysis of a generalized Gause model with prey harvesting and a generalized Holling response function of type III, J. Differential Equations 249 (2010) 2316–2356.
[12] K.P. Hadeler, P. van den Driessche, Backword bifurcation in epidemic control, Math. Biosci. 146 (1997) 15–35.

[13] W. Liu, Simon A. Levin, Y. Iwasa, Influence of nonlinear incidence rates upon the behavior of SIRS epidemiological models, J. Math. Biol. 23 (1986) 187–204.
[14] W. Liu, H.W. Hethcote, S.A. Levin, Dynamical behavior of epidemiological models with nonlinear incidence rates, J. Math. Biol. 25 (1987) 359–380.
[15] J. Mena-Lorca, H.W. Hethcote, Dynamic models of infectious disease as regulators of population sizes, J. Math. Biol. 30 (1992) 693–716.
[16] S. Ruan, W. Wang, Dynamical behavior of an epidemic model with a nonlinear incidence rate, J. Differential Equations 188 (2003) 135–163.
[17] C. Shan, H. Zhu, Bifurcations and complex dynamics of an SIR model with the impact of the number of hospital beds, J. Differential Equations 257 (2014) 1662–1688.
[18] Y. Tang, D. Huang, S. Ruan, W. Zhang, Coexistence of limit cycles and homoclinic loops in a SIRS model with a nonlinear incidence rate, SIAM J. Appl. Math. 69 (2008) 621–639.
[19] P. van den Driessche, J. Watmough, Reproduction numbers and sub-threshold endemic equilibria for compartmental models of disease transmission, Math. Biosci. 180 (2002) 29–48.
[20] D. Xiao, Bifurcations of saddle singularity of codimension three of a planar vector field with nilpotent linear part, Sci. China Ser. A 23 (1993) 252–260.
[21] World Health Organization, World health statistics, 2005–2014.
[22] D. Xiao, K.F. Zhang, Multiple bifurcations of a predator–prey system, Discrete Contin. Dyn. Syst. Ser. B 8 (2007) 417–433.
[23] H. Zhu, S. Campbell, G. Wolkowicz, Bifurcation analysis of a predator–prey system with nonmonotonic functional response, SIAM J. Appl. Math. 63 (2002) 636–682.
[24] H. Zhu, C. Rousseau, Finite cyclicity of graphics with a nilpotent singularity of saddle or elliptic type, J. Differential Equations 178 (2002) 325–436.